

University of Groningen

Comparative transcriptomics and metabolomics reveal specialized metabolite drought stress responses in switchgrass (*Panicum virgatum* L.)

Tiedge, Kira Juliane; Li, Xingxing; Merrill, Amy; Davisson, Danielle; Chen, Yuxuan ; Yu, Ping; Tantillo, Dean ; Last, Robert L. ; Zerbe, Philipp

Published in:
 bioRxiv

DOI:
[10.1101/2022.04.20.488672](https://doi.org/10.1101/2022.04.20.488672)

IMPORTANT NOTE: You are advised to consult the publisher's version (publisher's PDF) if you wish to cite from it. Please check the document version below.

Document Version
 Early version, also known as pre-print

Publication date:
 2022

[Link to publication in University of Groningen/UMCG research database](#)

Citation for published version (APA):

Tiedge, K. J., Li, X., Merrill, A., Davisson, D., Chen, Y., Yu, P., Tantillo, D., Last, R. L., & Zerbe, P. (2022). Comparative transcriptomics and metabolomics reveal specialized metabolite drought stress responses in switchgrass (*Panicum virgatum* L.). Manuscript submitted for publication.
<https://doi.org/10.1101/2022.04.20.488672>

Copyright

Other than for strictly personal use, it is not permitted to download or to forward/distribute the text or part of it without the consent of the author(s) and/or copyright holder(s), unless the work is under an open content license (like Creative Commons).

The publication may also be distributed here under the terms of Article 25fa of the Dutch Copyright Act, indicated by the "Taverne" license. More information can be found on the University of Groningen website: <https://www.rug.nl/library/open-access/self-archiving-pure/taverne-amendment>.

Take-down policy

If you believe that this document breaches copyright please contact us providing details, and we will remove access to the work immediately and investigate your claim.

Downloaded from the University of Groningen/UMCG research database (Pure): <http://www.rug.nl/research/portal>. For technical reasons the number of authors shown on this cover page is limited to 10 maximum.

1 **Comparative transcriptomics and metabolomics reveal specialized metabolite drought stress**
2 **responses in switchgrass (*Panicum virgatum* L.)**

3

4 Kira Tiedge^{1,2}, Xingxing Li^{3,4}, Amy T. Merrill⁵, Danielle Davisson¹, Yuxuan Chen¹, Ping Yu⁶,
5 Dean J. Tantillo⁵, Robert L. Last^{3,4,7}, Philipp Zerbe^{1*}

6

7 ¹Department of Plant Biology, University of California, Davis, CA, USA

8 ²Groningen Institute for Evolutionary Life Sciences, University of Groningen, The Netherlands

9 ³Department Biochemistry and Molecular Biology, Michigan State University, MI, USA

10 ⁴DOE Great Lakes Bioenergy Research Center, Michigan State University, MI, USA

11 ⁵Department of Chemistry, University of California, Davis, CA, USA

12 ⁶NMR Facility, University of California, Davis, CA, USA

13 ⁷Department Plant Biology, Michigan State University, MI, USA

14 *To whom correspondence should be addressed: Philipp Zerbe; email: pzerbe@ucdavis.edu;

15 phone: (530) 754-9652; ORCID ID: 0000-0001-5163-9523

16

17

18

19

20 SUMMARY

- 21 • Switchgrass (*Panicum virgatum*) is a bioenergy model crop valued for its energy efficiency
22 and drought tolerance resilience. The related monocot species rice (*Oryza sativa*) and
23 maize (*Zea mays*) deploy species-specific, specialized metabolites as core stress defenses.
24 By contrast, specialized chemical defenses in switchgrass are largely unknown.
- 25 • To investigate specialized metabolic drought responses in switchgrass, we integrated
26 tissue-specific transcriptome and metabolite analyses of the genotypes Alamo and Cave-
27 in-Rock that feature different drought tolerance.
- 28 • The more drought-susceptible Cave-in-Rock featured an earlier onset of transcriptomic
29 changes and significantly more differentially expressed genes in response to drought
30 compared to Alamo. Specialized pathways showed moderate differential expression
31 compared to pronounced transcriptomic alterations in carbohydrate and amino acid
32 metabolism. However, diterpenoid-biosynthetic genes showed drought-inducible
33 expression in Alamo roots, contrasting largely unaltered triterpenoid and phenylpropanoid
34 pathways. Metabolomic analyses identified common and genotype-specific flavonoids and
35 terpenoids. Consistent with transcriptomic alterations, several root diterpenoids showed
36 significant drought-induced accumulation, whereas triterpenoid abundance remained
37 predominantly unchanged. Structural analysis of drought-responsive root diterpenoids
38 verified these metabolites as oxygenated furanoditerpenoids.
- 39 • Drought-dependent transcriptome and metabolite profiles provide the foundation to
40 understand the molecular mechanisms underlying switchgrass environmental resilience.
41 Accumulation of specialized root diterpenoids and corresponding pathway transcripts
42 supports a role in drought stress tolerance for these compounds.

43 **Significance statement**

44 With an increasing demand for renewable energy opposed by rising climate-driven crop losses,
45 understanding, and leveraging plant natural defenses can enable the development of sustainable
46 crop production systems. Here, we integrated comparative transcriptomics and metabolomics
47 analyses to gain a detailed understanding of the diversity and physiological relevance of
48 specialized metabolites in upland and lowland switchgrass ecotypes and provide resources for
49 future investigations of drought response mechanisms in switchgrass.

50

51 **Keywords**

52 Drought stress; *Panicum virgatum* (switchgrass); plant specialized metabolism; natural products;
53 transcriptomics; metabolomics; diterpenoids; bioenergy crops

54

55

56

57

58

59

60

61

62

63 **Introduction**

64 Water scarcity exacerbated by climate change threatens biofuel and food crop production across
65 the world (Pokhrel et al. 2021; Challinor et al. 2014; Kim et al. 2019b). In the U.S., about one-
66 third of all counties are currently designated as crop loss disaster areas through drought by the U.S.
67 Department of Agriculture (USDA Farm Service Agency, 2021). Crop production is further
68 impacted by climate-associated increases in pest and pathogen damage (Newbery et al. 2016),
69 calling for new solutions to develop crops that can withstand current and future climate conditions.

70 The perennial grass switchgrass (*Panicum virgatum*) is a characteristic species of North American
71 tallgrass prairie land and of agro-economic value as a C₄ lignocellulosic feedstock (McLaughlin et
72 al. 1999). A high net-energy yield and environmental resilience make switchgrass economically
73 viable for biofuel production on marginal lands with reduced agricultural inputs. Two major
74 switchgrass ecotypes, Northern upland and Southern lowland, differ in climatic and geographical
75 adaptation, morphological characteristics and genetic architecture (Ayyappan et al. 2017; Lowry
76 et al. 2014). Upland ecotypes are mostly octoploid ($2n=8x=72$), whereas lowland ecotypes are
77 predominantly tetraploid ($2n=4x=36$) and feature taller phenotypes with thicker stems and a later
78 flowering time (Casler et al. 2011). The recent development of genome resources for the
79 allotetraploid lowland ecotype Alamo (~1.23 Gb, NCBI:txid38727) (Lovell et al. 2021) now
80 provides the foundation needed to investigate genetic and biochemical mechanisms underlying
81 switchgrass environmental resilience. Indeed, genomic analysis of 732 switchgrass genotypes
82 across 1,800 km latitude range revealed an extensive correlation of genomic architecture to
83 climatic adaptation (Lovell et al. 2021). Comparative morphological and physiological analysis of
84 49 upland and lowland ecotypes showed significant differences in the drought tolerance of
85 different switchgrass ecotypes (Liu et al. 2015). Large-scale transcriptomic changes were also

86 observed, including a drought-induced down-regulation of photosynthetic genes, consistent with
87 physiological responses such as reduced leaf water potential, reduced chlorophyll, and other
88 photosynthetic metabolites (Meyer et al. 2014; Lovell et al. 2016; Liu et al. 2015). Comparative
89 analysis of rhizosheath metabolites further showed an increase in amino acids, carbohydrates and
90 organic acids in response to drought (Liu et al. 2019).

91 In contrast, knowledge of the contribution of specialized metabolites to switchgrass stress response
92 mechanisms has remained largely unexplored. For example, drought-induced alterations in
93 terpenoid and phenylpropanoid metabolism have been reported (Meyer et al. 2014). In addition,
94 our prior work revealed an expansive network of terpenoid-metabolic *terpene synthase* (*TPS*) and
95 *cytochrome P450 monooxygenase* (*P450*) genes in *P. virgatum* var. Alamo, and combined
96 metabolite and transcript profiling illustrated the formation of species-specific diterpenoids and
97 the corresponding biosynthetic genes in switchgrass leaves and roots exposed to UV radiation and
98 oxidative stress (Pelot et al. 2018; Muchlinski et al. 2019; Tiedge et al. 2020). Furthermore,
99 emission of volatile mono- and sesqui-terpenoids was observed from switchgrass leaves and roots
100 upon herbivore stress and treatment with defense-related plant hormones (Muchlinski et al. 2019).
101 These collective insights support the importance of terpenoids and other specialized metabolite
102 classes for switchgrass abiotic and biotic stress tolerance. Recent maize (*Zea mays*) and rice (*Oryza*
103 *sativa*) studies showing induced diterpenoid formation under UV, oxidative and drought stress and
104 decreased abiotic stress tolerance in diterpenoid-deficient maize mutants support a broader role of
105 terpenoids in abiotic stress adaptation in monocot crops (Schmelz et al. 2014; Ding et al. 2021;
106 Park et al. 2013; Horie et al. 2015; Vaughan et al. 2015a).

107 A deeper understanding of the relevance of specialized metabolism in drought tolerance
108 and more broadly climatic adaptation in perennial biofuel crops can provide resources to improve

109 breeding strategies for developing locally and broadly adapted feedstock systems (Morrow et al.
110 2014). In this study, we integrated tissue-specific transcriptome and metabolite analyses to
111 investigate specialized metabolism responses to drought in two major switchgrass ecotypes with
112 distinct habitats and contrasting drought tolerance (Liu et al. 2015), namely the lowland Alamo
113 and the upland Cave-in-Rock genotypes.

114

115 **Results**

116 To investigate metabolic drought responses in switchgrass, we selected the lowland genotype
117 Alamo (AP13) and the upland genotype Cave-in-Rock which were ranked among the most
118 drought-tolerant and drought-susceptible genotypes in a comparative study of 49 switchgrass
119 varieties (Liu et al. 2015). At the beginning of the reproductive stage (R1), plants were exposed to
120 four weeks of continuous drought treatment, whereby soil water content measured as Available
121 Water Capacity (AWC) remained stable at 75% in well-watered control plants and decreased from
122 75% to 0% in drought-stressed plants (Supporting Information Fig. S1). Leaf and root tissue of
123 both genotypes and treatment groups was harvested before the treatment (week 0), after two weeks
124 and after four weeks, and samples were subject to transcriptomic and metabolomic analyses.
125 Between three and four weeks of drought treatment Cave-in-Rock plants displayed an increasing
126 wilting phenotype, whereas Alamo plants showed no or only minor wilting throughout the four-
127 week drought treatment (Fig. 1).

128

129 *Alamo and Cave-in-Rock plants show distinct transcriptomic alterations in response to drought*

130 Illumina Novaseq 6000 RNA sequencing yielded a total of 2.4 billion and 2.7 billion high-quality
131 reads for Alamo and Cave-in-Rock samples, respectively, representing >97% of the total reads
132 obtained in both datasets. Alignment of the high-quality sequences against the switchgrass Alamo
133 AP13 genome (phytozome-next.jgi.doe.gov/info/Pvirgatum_v5_1) resulted in average mapping
134 rates of 86% for Alamo and 83% for Cave-in-Rock, thus providing a comprehensive
135 transcriptomic dataset for gene discovery and gene expression analyses. Using this dataset,
136 differential gene expression analysis was performed for control and drought-treated plants of both
137 genotypes. A total of 565 differentially expressed genes (DEGs) were identified in roots and 204
138 DEGs in leaves (DEG threshold: $\text{padj} < 0.05$; $|\log_2 \text{FC}| > 1$) of Alamo plants after four weeks of
139 drought treatment compared to well-watered control plants (Fig. S2). Cave-in-Rock plants showed
140 stronger drought-induced changes with a total of 1198 DEGs in roots and 1120 DEGs in leaves;
141 constituting 2- and 5-fold more DEGs as compared to Alamo roots and leaves, respectively (Fig.
142 S2). In addition, Cave-in-Rock plants showed an earlier onset of transcriptomic changes compared
143 to Alamo. After two weeks of watering withdrawal, 2951 and 897 genes were differentially
144 expressed in Cave-in-Rock leaves and roots, respectively, whereas only 19 and 128 genes were
145 differentially expressed in Alamo leaves and roots (Supporting Information Table S1), concurrent
146 with the earlier onset of phenotypic drought symptoms in Cave-in-Rock (Fig. S2). Furthermore,
147 differential gene expression was more pronounced in roots than leaves in both genotypes. Indeed,
148 permutational multivariate analysis of variance (PERMANOVA) illustrated that tissue type
149 (leaves or roots) had the predominant impact on gene expression levels (38.6%, $p < 0.001^{***}$),
150 followed by genotype (8%, $p < 0.003^{**}$) and stress treatment (6%, $p < 0.007^{**}$) (Supporting
151 Information Table S2).

152

153 ***Major transcriptomic changes include genes of known drought response mechanisms and core***
154 ***general metabolic processes***

155 Consistent with the differences in the number and onset of DEGs between Alamo and Cave-in-
156 Rock, the identified genes showing the most significant differential expression differed between
157 the two genotypes and tissues (Fig. 1). Only two genes, a putative circadian clock protein
158 (*Pavir.9NG553200*) and a predicted lipid transfer protein (*Pavir.5NG603383*) were differentially
159 expressed in all genotypes and tissues (Fig. S2). The genotype- or tissue-specific DEGs included
160 numerous so far uncharacterized genes as well as several genes associated with known drought
161 response mechanisms. For example, in roots of both genotypes *dehydrin* ($\log_2(\text{fold change})$
162 Alamo=5.2, CiR=6.24) and other *Late Embryogenesis Abundant (LEA)* genes ($\log_2(\text{fold change})$
163 Alamo=4.34, CiR=5.78), as well as several *AWPM19-like* plasma-membrane-associated abscisic
164 acid (ABA) influx transporters implicated with drought tolerance ($\log_2(\text{fold change})$ Alamo=6.25,
165 CiR=6.04) were highly upregulated (Fig. 1, Supporting Information Table S1). Notably, among
166 the 11 *AWPM19-like* genes, Alamo and Cave-in-Rock featured distinct genes (*Pavir.2NG274300*
167 in Alamo versus *Pavir.9NG018700* in Cave-in-Rock) as the most differentially expressed
168 *AWPM19-like* genes. The increased expression of known drought-associated genes supports the
169 drought response in both genotypes, despite the visual lack of a wilting phenotype in Alamo plants.

170 Next, we investigated the impact of drought on core metabolic pathways independent of known
171 drought response processes. Among 26 GO terms significantly enriched in all samples combined
172 most encoded for biological processes or molecular functions (Fig. S3). In Alamo leaves DNA-
173 binding and electron carrier processes were most significantly enriched, whereas carbohydrate
174 metabolism was predominant in roots. Interestingly, Cave-in-Rock roots featured highly enriched
175 abiotic stress response processes rather than carbohydrate metabolism under drought stress,

176 whereas leaves showed patterns similar to Alamo with DNA-binding and hydrolase activities
177 being differentially expressed (Fig. S3). Additional pathway enrichment analyses using KEGG
178 terms confirmed a substantially higher number of metabolic pathways enriched in Cave-in-Rock
179 as compared to Alamo, with more genes underlying the enriched pathways on average (Fig. 2 and
180 Fig. S4). Plant signal transduction process ranked among the most significantly enriched in Alamo
181 and Cave-in-Rock leaves, especially in response to drought stress. By contrast, endoplasmic
182 reticulum protein processing and nitrogen metabolism were most significantly altered in Alamo
183 and, to lesser degree, in Cave-in-Rock roots (Fig. 2). Albeit at lower levels, pathway enrichment
184 was also observed for general and specialized metabolism, including carbon and amino acid
185 metabolism, as well as carotenoid, steroid, and phenylpropanoid biosynthesis (Fig. 2, Supporting
186 Information Table S3).

187

188 ***Switchgrass features tissue-, genotype- and drought-specific alterations in terpenoid and***
189 ***phenylpropanoid pathways***

190 The enrichment of terpenoid and phenylpropanoid metabolism is consistent with prior studies
191 illustrating the up-regulation, albeit at moderate levels, of switchgrass terpenoid- and
192 phenylpropanoid-metabolic pathways in response to drought, UV irradiation and oxidative stress
193 (Meyer et al. 2014; Pelot et al. 2018; Muchlinski et al. 2019; Tiedge et al. 2020). To investigate in
194 more detail the impact of drought on switchgrass specialized metabolism, we compared the
195 transcript abundance of key genes of the terpenoid and phenylpropanoid scaffold-forming
196 pathways in both genotypes. Due to the lack of a Cave-in-Rock genome, gene annotations are
197 based on homology searches against the switchgrass Alamo AP13 genome (phytozome-
198 next.jgi.doe.gov/info/Pvirgatum_v5_1). Interestingly, the focal genes showed similar tissue-

199 specific expression profiles in Alamo and Cave-in-Rock and no substantial drought-induced gene
200 expression changes were observed (Fig. 3). For example, of the four annotated *1-deoxyxylulose 5-*
201 *phosphate synthase (DXS)* genes of the methylerythritol phosphate (MEP) pathway, two
202 homologs, *Pavir.3KG128241* and *Pavir.3NG140939*, were abundant in leaves but ~10-60-fold less
203 in roots of both Alamo and Cave-in-Rock (Fig.3a). Likewise, the predicted squalene synthase,
204 *Pavir.4NG340500*, displayed high abundance in leaves and low gene expression in roots.
205 However, select genes showed genotype-specific differences in their expression patterns. This
206 included the predicted *geranylgeranyl pyrophosphate synthase (GGPPS)*, *Pavir.6Ng089000*, that
207 was expressed in Alamo but not Cave-in-Rock roots (Fig. 3a). A similar trend of gene expression
208 was observed for core genes of phenylpropanoid metabolism with several annotated *phenylalanine*
209 *ammonia lyase (PAL)*, *cinnamate-4-hydroxylase (C4H)*, and *4-coumaroyl-CoA ligase (4CL)* genes
210 showing higher expression in roots as compared to leaves in both Alamo and Cave-in-Rock (Fig.
211 3b).

212 Contrasting the largely unaltered and comparable expression of the highly conserved upstream
213 pathway genes, both Alamo and Cave-in-Rock plants featured distinct gene expression profiles for
214 downstream pathway branches that generate species-specific, functionalized metabolites.
215 Following the recent discovery of specialized triterpenoid and steroid saponins in switchgrass (Li
216 et al. 2020), identification and gene expression analysis of predicted *cycloartenol synthases (CAS)*,
217 *lanosterol synthases (LAS)*, *β -amyrin synthases (BAS)*, as well as members of the *CYP71A*,
218 *CYP90B* and *CYP94D* cytochrome P450 families and *sterol 3- β -glucosyltransferases* with known
219 functions in triterpenoid metabolism revealed distinct expression patterns across tissue type and
220 genotype (Fig. 4). For example, hierarchical gene cluster analysis illustrated predicted *triterpenoid*
221 *synthase (TTS)* genes and a putative *CYP72A* gene with similar inducible expression patterns in

222 Alamo leaves after two and four weeks of drought (Supporting Information Table S4). Likewise,
223 in Alamo roots a different group of *TTS*, *sterol 3- β -glucosyltransferase*, and putative *CYP72A*,
224 *CYP94D* and *CYP90B* genes, known to function in the biosynthesis of triterpenoid saponins such
225 as diosgenin (Ciura et al. 2017), displayed common inducible expression patterns after four weeks
226 of drought (Fig. 4 upper panel). By contrast, co-expression patterns of triterpenoid-biosynthetic
227 genes were not detectable in Cave-in-Rock (Fig. 4 lower panel).

228 Our prior research identified expansive, species-specific diterpene synthase (diTPS) and P450
229 families in switchgrass that form complex metabolic networks toward a range of labdane-related
230 diterpenoids, including *syn*-pimarane and furanoditerpenoid compounds that occur, perhaps
231 uniquely, in switchgrass (Fig. S5) (Pelot et al. 2018; Muchlinski et al. 2021). This pathway
232 knowledge enabled a detailed analysis of transcriptomic alterations related to diterpenoid
233 metabolism. Contrasting the largely similar expression patterns of MEP and MVA pathway genes
234 (Fig. 3a), hierarchical gene cluster analysis revealed distinct *diTPS* and *P450* gene expression
235 between Alamo and Cave-in-Rock (Fig. 5). In Alamo roots, the *cis-trans-clerodienyl*
236 *pyrophosphate (CLPP) synthase PvCPS1* and the *P450* genes, *CYP71Z25*, *CYP71Z26*, and
237 *CYP71Z28* shown to form furanoditerpenoids (Muchlinski et al. 2021), showed patterns of co-
238 expression at two and four weeks of drought. Similarly, the predicted *syn*-*CPP synthases*, *PvCPS9*
239 and *PvCPS10*, as well as two class I diTPS, *PvKSL4* and *PvKSL5*, shown to form *syn*-pimaradiene
240 compounds (Pelot et al. 2018), co-expressed in roots, albeit without significant drought-inducible
241 transcript changes. In Cave-in-Rock, *diTPS* and *P450* genes were expressed mostly in the well-
242 watered plants and water deficiency did not elicit significant transcript accumulation. Also,
243 contrasting roots, no drought-elicited changes in the expression of diterpenoid pathway genes was
244 detectable in leaves of either ecotype.

245

246 ***Switchgrass leaves and roots show drought-inducible metabolite alterations***

247 To complement transcriptomic studies leaf and root metabolomes of Alamo and Cave-in-Rock
248 plants under drought-stressed and well-watered conditions were examined using untargeted liquid-
249 chromatography-quadrupole Time of Flight-mass spectrometry (LC-QToF-MS) analysis. Using
250 accurate mass, retention time (RT), and fragmentation patterns, we identified 5181 and 3234
251 metabolite features in positive and negative ion mode, respectively. To compare metabolite
252 profiles across tissues, genotypes and treatments, after filtering for ion-abundance (see Methods)
253 2519 positive mode mass features (identified as retention time- m/z ratio pairs) were selected for
254 downstream statistical analysis (Supporting Information Table S5).

255 Aligned with the transcriptomic changes, biostatistical analysis of the untargeted metabolomic data
256 via PERMANOVA showed that tissue type had the highest impact on metabolite composition
257 (72.4%, $p < 0.001$ ***), followed by difference in genotype (2.8%, $p < 0.028$ *) and drought-treatment
258 versus control (0.6%, $p < 0.332$) (Supporting Information Table S2). Hence, we further analyzed
259 the metabolite profiles independently within each tissue type. Despite the relatively lower impact
260 of drought treatment on metabolic alterations, under a multivariate dimension-reduction based on
261 genotype metabolite features clustered together prior to water deprivation (week 0), but separated
262 in leaves and, to a lesser extent, in roots after four weeks of drought treatment (Fig. 6). This shift
263 in metabolite composition was driven by several major features (Fig. 7). In leaves, most
264 compounds showing accumulation differences in control and drought-stressed plants were
265 annotated as phospholipids based on database searches for each feature. These compounds
266 increased in abundance in Alamo during drought treatment, whereas a decrease was observed in
267 Cave-in-Rock (Fig. 7). In addition to predicted phospholipids, a few features were enriched in

268 Alamo leaves under drought stress, whereas many unidentified compounds were enriched in
269 drought-treated Cave-in-Rock leaves (Supporting Information Table S2). In contrast, several
270 compounds identified as diterpenoids and triterpenoids by comparison of RT and fragmentation
271 patterns to previously identified compounds (Li et al., 2020; Muchlinski et al., 2021) accumulated
272 in roots of both Alamo and Cave-in-Rock plants under drought stress, with a stronger increase in
273 Alamo (Fig. 7). Other root metabolites that accumulated differentially under drought conditions
274 either did not score significant database matches or could only be assigned to the general classes
275 of carbohydrates, acids, or alcohols (Fig. 7). Among the few features that were generally enriched
276 in both leaves and roots and in both ecotypes under water deficient conditions was also abscisic
277 acid (ABA), which was increased by ~40-300-fold under drought (Fig. 8a, Supporting Information
278 Table S6, ABA: 6.08_247.1244m/z).

279 ***Drought induces the accumulation of specialized furanoditerpenoids in switchgrass roots***

280 Considering that predicted specialized steroidal and triterpenoid saponins and diterpenoids
281 contribute substantially to the metabolic differences between Alamo and Cave-in-Rock roots, we
282 examined these compounds in more detail in leaf and root extracts after four weeks of drought
283 where the physiological stress symptoms were most pronounced. Several predicted flavonoid
284 glycosides were identified in leaves of Alamo and Cave-in-Rock plants but were absent in root
285 tissue. However, these compounds showed no or only minimal patterns of drought-elicited
286 accumulation (Fig. 8a). In addition, a range of distinct terpenoid metabolites was identified.
287 Among these metabolites, the largest group represented recently identified steroidal or triterpenoid
288 saponins (Li et al. 2020), showing distinct profiles across tissues and genotypes. Triterpenoid
289 saponins occurred predominantly in leaves of both Alamo and Cave-in-Rock plants, whereas the
290 larger group of steroidal saponins were present in leaves and/or roots and occurred predominantly

291 in either Alamo or Cave-in-Rock plants. Despite the overall abundance of these saponins, the vast
292 majority of the annotated metabolites were not significantly enriched upon drought stress ($p \leq$
293 0.05, Supporting Information Table S6). In addition to the larger group of triterpenoids, 11
294 compounds predicted as specialized diterpenoids were identified, the majority of which occurred
295 predominantly in Alamo roots and were absent or abundant at only low levels in Cave-in-Rock
296 (Fig. 8a). Notably, two pairs of predictably isomeric diterpenoids were detected in Alamo and
297 Cave-in-Rock that showed substantial accumulation mostly in drought-stressed roots. One
298 metabolite pair at retention times of 9.06 min and 9.26 min featured a dominant precursor mass
299 ion of m/z 317 $[M+H]^+$ and one compound pair at retention times of 11.50 min and 11.72 min
300 featured a dominant ion of m/z 317 $[M+H]^+$. Together with the presence of additional mass ions
301 of m/z 257, m/z 189, m/z 177 or m/z 135, these fragmentation patterns suggested that these
302 compounds represent labdane-related diterpenoids carrying one or more oxygenation functions
303 (Supporting Information Fig. S4). To elucidate the precise structure of these diterpenoids,
304 metabolites were extracted from mature Cave-in-Rock roots and purified via liquid-liquid phase
305 partitioning followed by HPLC. Purified samples (0.4-0.8 mg for each compound) of both m/z 301
306 isomers and both m/z 317 diterpenoid isomers were used for 1D (1H and ^{13}C) and 2D (HSQC,
307 COSY, HMBC and NOESY) NMR analyses. Collectively, the generated data identified the m/z
308 301 diterpenoids as 15,16-epoxy-2-oxo-5 α 8 α -cleroda-3,13(16),14-triene and its C19 enantiomer,
309 while the earlier eluting diterpenoid m/z 317 was identified as 2-oxo-5 α 8 α -cleroda-3,13-dien-
310 16,15-olide, together designated as panicoloid A,B, and C respectively (Fig. 8b, Supporting
311 Information Fig. S6). Insufficient abundance and purity of the later eluting m/z 317 diterpenoid
312 isomer prevented structural analysis of this metabolite. Based on the similar mass fragmentation
313 pattern and retention time compared to the other m/z 317 isomer (Supporting Information Fig. S4),

314 it is plausible that this compound represents its enantiomeric isomer and is tentatively named
315 panicoid D. The identified diterpenoids represent derivatives of previously identified
316 switchgrass furanoditerpenoids that feature additional carbonyl functions at C2 and/or C14 and are
317 collectively named here as the group of panicoids (Fig. S4).

318

319 **Discussion**

320 Knowledge of the gene-to-metabolite relationships underlying specialized metabolic pathways
321 that contribute to plant stress resilience can enable new crop optimization strategies for addressing
322 exacerbating environmental pressures and associated harvest loss (Savary et al. 2019). Extensive
323 studies in major food and bioenergy crops such as rice, maize, and sorghum (*Sorghum bicolor*)
324 have demonstrated that species-specific blends of specialized terpenoids, phenylpropanoids,
325 oxylipins, and benzoxazinoids mediate complex responses to biotic and abiotic perturbations
326 (Schmelz et al. 2014; Murphy and Zerbe 2020). By contrast, knowledge of the diversity of
327 specialized metabolites in the perennial bioenergy crop switchgrass and its relevance for drought
328 adaptation in different switchgrass genotypes is incomplete. Combined transcriptome and
329 metabolome analysis of the lowland ecotype Alamo shown to be drought-tolerant and the upland
330 ecotype Cave-in-Rock with low drought tolerance (Liu et al. 2015) revealed common and distinct
331 metabolic alterations and identified specialized diterpenoid metabolites with possible functions in
332 switchgrass drought adaptation.

333 Consistent with prior studies showing that upland and lowland switchgrass ecotypes have different
334 transcriptomic profiles under optimal conditions (Ayyappan et al. 2017), this study demonstrates
335 that metabolic alterations in Alamo and Cave-in-Rock are predominantly driven by differences in

336 tissue type and genotype, thus reflecting the different habitat range and climatic adaptation of
337 switchgrass ecotypes. A stronger wilting phenotype after four weeks of drought treatment, along
338 with more than twice as many differentially expressed genes illustrate more pronounced drought-
339 induced metabolic changes in Cave-in-Rock, consistent with prior studies identifying Cave-in-
340 Rock as particularly drought-susceptible among switchgrass varieties (Liu et al. 2015). Presence
341 of known drought-response genes among the most differentially expressed genes in Alamo and/or
342 Cave-in-Rock supported substantial drought responses in both genotypes during drought
343 treatment, despite the lack of significant phenotypic changes in Alamo. Known drought-associated
344 genes included *LEA* genes, including dehydrin shown to impact drought tolerance in *Arabidopsis*
345 and cotton (*Gossypium spec.*) (Olvera-Carrillo et al. 2010; Magwanga et al. 2018), a NAC
346 transcription factor (*Pavir.8KG003520*) shown to contribute to drought tolerance in a recent
347 switchgrass GWAS study (Lovell et al. 2021), and AWPM-19-like abscisic acid (ABA) influx
348 transporters (Yao et al. 2018). Differential expression of several AWPM-19-like genes in both
349 Alamo and Cave-in-Rock is consistent with an increase in ABA observed in both genotypes and
350 tissues in response to drought stress. While prior studies that showed increased ABA and sugar
351 accumulation in drought-tolerant switchgrass genotypes (Liu et al. 2015), the final concentration
352 of ABA in drought stressed plants was at comparable levels in both genotypes in our study,
353 whereas the concentration in the control plants was lower in Alamo, resulting in a higher fold-
354 change/increase in Alamo when compared to Cave-in-Rock. Notably, the specific genes of the
355 above gene families being differentially expressed differed between Alamo and Cave-in-Rock,
356 suggesting that switchgrass genotypes recruit specific genes governing stress response
357 mechanisms.

358 Pathways of general and specialized metabolism showed overall comparatively moderate
359 differential gene expression in response to drought stress with apparent metabolic differences
360 between leaf and root tissue. Accumulation of sucrose and ABA in Alamo and Cave-in-Rock
361 tissues is consistent with previously demonstrated switchgrass drought responses (Liu et al. 2015).
362 In addition, the observed major contribution of phospholipids to metabolic alterations in leaves of
363 both genotypes may be related to an upregulation of pathways involved in membrane lipid systems
364 and cell wall biosynthesis as shown in, for example, drought-resistant maize lines (Zhang et al.
365 2020). Additional phospholipid roles in drought tolerance may include maintenance of membrane
366 integrity or mitigation of drought-related cell damage (Hamrouni et al. 2001), as well as signaling
367 processes during water deficiency as reported in selected drought-resistant species (Moradi et al.
368 2017; Quartacci et al. 1995). Contrasting drought-related flavonoid functions in, for example,
369 wheat (*Triticum aestivum*) and other species (Gai et al. 2020; Ma et al. 2014), leaf flavonoid
370 glycosides did not accumulate in response to drought in either switchgrass genotype, despite a
371 moderate upregulation of select pathway genes such as *CHS* in drought-stressed plants. Similarly,
372 steroidal and triterpenoid saponins were identified in switchgrass leaves, and have been shown to
373 increase as part of the leaf cuticular waxes in response to drought (Kim et al. 2007). However, our
374 metabolite analysis did not show significant drought-elicited triterpenoid accumulation that would
375 support a similar function in switchgrass.

376 Different from leaves, steroidal and other triterpenoid saponins as well as diterpenoids constituted
377 the major determinants of metabolic differences in drought-stressed roots. Notably, MEP and
378 MVA pathway genes showed no or very minor patterns of drought-inducible expression in Alamo
379 or Cave-in-Rock, indicating that no major change in the production of terpenoid precursors occurs
380 in response to drought. One exception is the putative *GGPPS*, *Pavir.6NG089000*, that is expressed

381 in Alamo but not Cave-in-Rock roots and may contribute to differences in terpenoid metabolism
382 between these genotypes. This apparent lack of drought activation of terpenoid backbone pathways
383 suggests that terpenoid accumulation has to derive from existing precursor pools via changes in
384 pathway branches en route to specific terpenoids. Indeed, in leaves and roots of Alamo, but not
385 Cave-in-Rock, downstream triterpenoid-metabolic pathway genes increased under drought
386 conditions. Interestingly, no apparent triterpenoid-biosynthetic gene clusters were identified in the
387 switchgrass genome, which differentiates switchgrass from other plant species where triterpenoid
388 metabolism is commonly arranged in form of often stress-inducible biosynthetic clusters (Liu et
389 al. 2020; Bai et al. 2021). Despite the lack of apparent genomic clusters, clear co-expression
390 patterns were observed for several *TTS* genes as well as *sterol 3- β -glucosyltransferases* and *P450*
391 genes of the *CYP71A*, *CYP94D* and *CYP90B* families, thus supporting the presence of co-
392 expressed pathways toward specific triterpenoids. The identification of diverse mixtures of
393 diosgenin and closely related triterpenoid saponins in roots of several upland and lowland ecotypes
394 supports this hypothesis (Lee et al. 2009; Li et al. 2020). However, the annotated triterpenoid
395 metabolites were not significantly enriched in response to drought in either genotype, suggesting
396 that the inducible expression of triterpenoid pathways in Alamo is related to distinct drought-stress
397 responses. It can be speculated that root triterpenoids serve antioxidant functions to mitigate
398 oxidative damage caused by water deficiency as shown in *Arabidopsis* and other species (Posé et
399 al. 2009; Nasrollahi et al. 2014; Puente-Garza et al. 2017). Also, recent studies have demonstrated
400 bioactive triterpenoids in roots exudates of soybean (*Glycine max*) and tomato (*Solanum*
401 *lycopersicum*) that aid the assembly of the root microbiome to confer robustness against
402 environmental stresses (Fujimatsu et al. 2020; Nakayasu et al. 2021). While distinct microbiome
403 responses to drought stress have been reported in upland and lowland switchgrass ecotypes (Liu

404 et al. 2021), the role of specialized metabolites such as saponins in these interactions is yet to be
405 discovered.

406 Unlike root triterpenoids, significant drought-induced accumulation of several diterpenoids in
407 roots supports a role in drought response mechanisms. Although requiring further biological
408 studies, the higher abundance of these diterpenoids in Alamo as compared to Cave-in-Rock may
409 contribute to the distinct stress resilience in these genotypes. In addition, accumulation in both
410 Alamo and Cave-in-Rock support a role of these metabolites in drought responses rather than
411 general stress responses associated with the more pronounced wilting phenotype observed in Cave-
412 in-Rock. Structural analysis identified three compounds as oxygenated clerodane
413 furanoditerpenoids, named here panicoloid A-C, which likely represent derivatives of
414 furanoditerpenoid scaffolds recently identified in switchgrass (Pelot et al. 2018; Muchlinski et al.
415 2021). Notably, the enantiomeric stereochemistry of panicoloid B and C is likely derived from the
416 activity of yet unidentified diTPS functionally related to the CLPP synthase PvCPS1. Drought-
417 induced gene expression increases of characterized pathway genes toward clerodane-type
418 furanoditerpenoids, including the diTPS *PvCPS1* and the P450 genes *CYP71Z25*, *CYP71Z26* and
419 *CYP71Z28* supports a role of these pathway genes in panicoloid biosynthesis. Additional co-
420 expression of select P450s of the CYP99 family and predicted short-chain alcohol
421 dehydrogenases/reductases, shown to function in specialized diterpenoid metabolism in maize and
422 rice (Swaminathan et al. 2009), suggests possible functions in the position-specific oxygenation
423 reactions toward panicoloid biosynthesis. Similar to triterpenoid metabolism, the lack of co-
424 expression of these genes in the drought-susceptible Cave-in-Rock genotype may support a role
425 of panicoloids in switchgrass drought responses. Combined with the abundance of yet unidentified
426 diterpenoids in switchgrass roots, drought-elicited co-expression patterns of additional predicted

427 *syn-CPP synthase* genes (*PvCPS9*, *PvCPS10*) and characterized class I diTPS forming *syn-*
428 pimarane diterpenoids (*PvKSL4*, *PvKSL5*) suggest the presence of a broader diversity of drought-
429 induced diterpenoids in switchgrass. Similar clerodane-type furanoditerpenoids have also been
430 identified in species of *Vellozia spec.* (Pinto et al. 1994), *Solidago spec.* (Anthonsen et al. 1973;
431 McCrindle et al. 1976), and *Croton campestris* (El Babili et al. 1998), where they will have evolved
432 independently given the phylogenetic distance between these plant genera. While the drought-
433 induced expression of diterpenoid-metabolic genes and associated accumulation of paniculoids
434 and possibly other diterpenoids supports a role in switchgrass drought tolerance, the underlying
435 mechanisms will require future investigation. However, drought-related diterpenoid bioactivities
436 have recently been supported in other monocots. For example, maize studies demonstrated the
437 accumulation of specialized kauralexin and dolabralexin diterpenoids in response to oxidative,
438 drought and salinity stress (Christensen et al. 2018; Mafu et al. 2018), and diterpenoid-deficient
439 maize mutants show decreased resilience to abiotic stress (Vaughan et al. 2015b). Additionally,
440 antioxidative functions in relation to drought stress have been shown for select diterpenoids
441 (Munné-Bosch and Alegre 2003), and diterpenoid roles in the root microbiome assembly have
442 been suggested based on changes in the microbiome composition in the kauralexin- and
443 dolabralexin-deficient maize *an2* mutant (Murphy et al. 2021).

444 Collectively, these findings exemplify the power of combining transcriptomic, metabolomic and
445 metabolite structural approaches to accelerate the discovery of plant specialized pathways and
446 products to better understand their relevance and role in plant stress responses. This approach
447 revealed common and distinct drought-induced metabolic changes in switchgrass genotypes of
448 contrasting drought tolerance. These insights provide the foundation for future targeted genetic

449 studies to investigate the diversity and protective function of terpenoids and other specialized
450 metabolites in switchgrass drought tolerance.

451

452 **Methods**

453 *Plant material and treatment*

454 Switchgrass genotypes Alamo AP13 and Cave-in-Rock were kindly provided by Dr. Malay Saha
455 (Noble Research Institute, USA). Plants were propagated from tillers to maintain low genetic
456 variation and cultivated in greenhouses to the reproductive stage (R1) under ambient photoperiod
457 and ~27/22°C day/night temperature prior to drought treatment in a random block design.
458 Following prior drought studies (Liu et al., 2015), drought stress was applied by withholding water
459 consecutively for four weeks, whereas control plants were watered daily. Volumetric soil water
460 content (SWC) was monitored regularly using a HydroSense II (Campbell Scientific, USA). Leaf
461 and root tissues of treated and control plants ($n=6$ per group) were collected before the start of the
462 treatment (week 0), after two weeks (week 2), and after four weeks (week 4) at a consistent time
463 and immediately flash-frozen in liquid N₂. To enable comparative data integration, samples for
464 transcriptome and metabolite analyses originated from the same plant tissue samples, which were
465 split for the different analyses.

466

467 *RNA isolation, transcriptome sequencing, and differential gene expression analysis*

468 Total RNA was extracted from 100 mg of leaves or roots of Alamo and Cave-in-Rock plants ($n=6$)
469 either drought-stressed or well-watered (control) using a Monarch[®] Total RNA Miniprep Kit (New

470 England Biolabs, USA) and subsequently treated with DNase I for genomic DNA removal.
471 Following assessment of RNA integrity and quantitation using the Bioanalyzer 2100 RNA Nano
472 6000 Assay Kit (Agilent Technologies Inc., CA, USA), four of the six biological replicates with
473 highest RNA quality were selected for sequencing. Preparation of cDNA libraries and
474 transcriptome sequencing was performed at Novogene (Novogene Corporation Inc., USA). In
475 brief, following RNA integrity analysis and quantitation, cDNA libraries were generated using a
476 NEBNext®Ultra™RNA Library Prep Kit (New England Biolabs, USA) and sequenced on an
477 Illumina Novaseq 6000 sequencing platform generating 40-80 million 150 bp paired-end reads per
478 sample. Filtered, high-quality reads were aligned to the reference genome (*P. virgatum* var. Alamo
479 AP13 v5.1) using HISAT2 (Kim et al. 2019a). Gene functional annotation was based on best
480 matches to databases from Phytozome v13 (phytozome-next.jgi.doe.gov), including Arabidopsis,
481 rice, Gene Ontology, and Panther, as well as in-house protein databases of biochemically verified
482 terpene-metabolic enzymes (Pelot et al. 2018; Murphy and Zerbe 2020). Differentially expressed
483 genes (DEGs) were identified based on $p_{adj} < 0.05$ and $|\log_2 FC| > 1$ as selection criteria. Statistical
484 analyses were conducted in R and also plots and heatmaps were created using the ‘ggplot2’ and
485 ‘pheatmap’ packages in R (cran-project.org, version 3.6.3).

486

487 ***Metabolite extraction***

488 Metabolite analysis followed previously established protocols (Li et al. (2020)). Here, 100 mg
489 tissue were ground to a fine powder in liquid N₂ and metabolites were extracted with 1 ml 80%
490 methanol containing 1 μM telmisartan internal standard by vortexing briefly and incubation for 16
491 h at 200 rpm and 4°C. Samples were centrifuged for 20 min (4000 g, 4°C) to remove solid particles
492 and the supernatants transferred into fresh vials and stored at -80°C prior to LC-MS analysis.

493

494 ***UPLC-ESI-QToF-MS analysis***

495 Metabolite profiling was achieved by reversed-phase Ultra Performance Liquid Chromatography-
496 Electrospray Ionization-Quadrupole Time-of-Flight mass spectrometry (UPLC-ESI-QToF-MS)
497 analysis in positive and negative ionization mode on a Waters Acquity UPLC system equipped
498 with a Waters Xevo G2-XS QToF MS (Waters, Milford, MA) and a Waters UPLC BEH C18 (1.7
499 μm x 2.1 mm x 150 mm) column. Chromatography was performed using 10 mM NH_4HCO_2 (in
500 water; solvent A) and 100% acetonitrile (solvent B) as mobile phase and the following parameters:
501 flow rate of 0.4 ml min^{-1} ; column temperature 40°C; 10 μl injection; method: 0-1 min (99% A/1%
502 B), 1-15 min linear gradient to 1% A/99% B, 15-18 min (1% A/99%B), 18-20 min (99% A/1%
503 B); QToF parameters: desolvation temperature of 350°C; desolvation gas flow rate at 600 L h^{-1} ;
504 capillary voltage of 3 kV; cone voltage of 30 V. Mass spectra were acquired in continuum mode
505 over m/z 50-1500 using data-independent acquisition (DIA) and MS^E with collision potential
506 scanned at 20-80 V for the higher energy function.

507 The obtained DIA MS data were processed using Progenesis QI (V3.0, Waters) for quality control,
508 chromatography alignment and mass feature extraction. Metabolite annotations were performed
509 by matching m/z ratios, RT and fragmentation patterns against metabolite databases through
510 Progenesis QI and LipidBlast (Kind et al. 2013). As a complimentary annotation approach, DDA
511 (data dependent acquisition) was performed on a subset of the samples to obtain MS/MS spectral
512 data for mainly the most abundant features. In addition, CANOPUS was used to predict chemical
513 classes of the features based on their MS/MS information (Dührkop et al. 2021). Ion abundances
514 of all detected features were normalized to the internal telmisartan standard based on five

515 biological replicates. The normalized data (abundance > 300) were used for statistical analysis
516 using MetaboAnalyst 5.0 (Pang et al. 2021).

517

518 *NMR analysis of terpenoid metabolites*

519 About 200 g fresh root tissues of Cave-in-Rock plants were harvested. Compound purification was
520 performed according to the method described in the Li et al (2020). The differences are the ethyl
521 acetate and hexane phases (in which the diterpenoids were concentrated) were evaporated to
522 dryness using a SpeedVac vacuum concentrator. The residue was re-dissolved in 8 mL of 95%
523 methanol. Supernatants were transferred to LC vials. Purification was carried out as previously
524 described using a C18 HPLC column (100 x 4,6 mm x 5µm). For NMR analysis, ~0.4-0.8 mg of
525 each HPLC purified compounds were dissolved in deuterated chloroform (CDCl₃; Sigma-Aldrich,
526 USA) containing 0.03% (v/v) tetramethylsilane (TMS). NMR 1D (¹H and ¹³C) and 2D (HSQC,
527 COSY, HMBC and NOESY) spectra were acquired as previously described (Pelot et al. 2018) on
528 a Bruker Avance III 800 MHz spectrometer (Bruker Corporation, MA, USA) equipped with a 5
529 mm CPTCI cryoprobe using Bruker TopSpin 3.6.1 software and analyzed with MestReNova 14.1
530 software. Chemical shifts were calibrated against known TMS signals.

531

532 **Acknowledgements**

533 We gratefully acknowledge Dr. Malay Saha at the Noble Research Institute for providing tillers
534 for cultivation of Alamo AP13 and Cave-in-Rock, Dr. Daniel A. Jones at Michigan State
535 University for his help with identification of diterpenoid features, and Dr. Andrew Muchlinski
536 (Firmenich, San Diego, USA) for helpful discussions on the manuscript.

537

538 **Author Contributions**

539 P.Z. and K.T. conceived the original research and oversaw data analysis; K.T. conducted plant
540 drought stress experiments and transcriptome analysis; X.L. performed metabolite profiling and
541 analysis; A.M., P.Y., and D.T. performed NMR structural analyses; D.D. and Y.C. assisted with
542 plant harvesting, sampling, and sample processing; K.T. and P.Z. wrote the original article draft
543 with editing by all authors. All authors have read and approved the manuscript.

544

545 **Data availability**

546 The RNA-seq data were submitted to the Sequence Read Archive (SRA), accession no.
547 PRJNA644234.

548

549 **Funding**

550 Financial support for this work was provided by the U.S. Department of Energy (DOE) Early
551 Career Research Program (DE-SC0019178, to PZ), the German Research Foundation (DFG)
552 Research Fellowship (TI 1075/1-1, to KT), and the DOE Joint Genome Institute (JGI) DNA
553 Synthesis Science Program (grant #2568, to PZ). The gene synthesis work conducted by the U.S.
554 Department of Energy Joint Genome Institute (JGI), a DOE Office of Science User Facility, is
555 supported by the Office of Science of the U.S. Department of Energy under Contract No. DE-
556 AC02-05CH11231. Work by X.L. and R.L.L. is supported by the Great Lakes Bioenergy Research
557 Center, U.S. Department of Energy, Office of Science, Office of Biological and Environmental

558 Research under Award Number DE-SC0018409.

559

560 **Conflict of interest statement**

561 The authors declare that they have no conflict of interest in accordance with the journal policy.

562

563 **References**

- 564 Agency UFS (2021) Secretarial Drought Designations for 2021. Washington, D.C.
- 565 Anthonson T, Henderson M, Martin A, Murray R, McCrindle R, McMaster D (1973) Constituents
566 of Solidago species. Part IV. Solidagoic acids A and B, diterpenoids from *Solidago*
567 *gigantea* var. *serotina*. Canadian Journal of Chemistry 51 (9):1332-1345
- 568 Ayyappan V, Saha MC, Thimmapuram J, Sripathi VR, Bhide KP, Fiedler E, Hayford RK,
569 Kalavacharla V (2017) Comparative transcriptome profiling of upland (VS16) and lowland
570 (AP13) ecotypes of switchgrass. Plant Cell Rep 36 (1):129-150. doi:10.1007/s00299-016-
571 2065-0
- 572 Bai Y, Fernández-Calvo P, Ritter A, Huang AC, Morales-Herrera S, Bicalho KU, Karady M,
573 Pauwels L, Buyst D, Njo M, Ljung K, Martins JC, Vanneste S, Beeckman T, Osbourn A,
574 Goossens A, Pollier J (2021) Modulation of *Arabidopsis* root growth by specialized
575 triterpenes. New Phytologist 230 (1):228-243. doi:10.1111/nph.17144
- 576 Casler MD, Tobias CM, Kaeppler SM, Buell CR, Wang Z-Y, Cao P, Schmutz J, Ronald P (2011)
577 The Switchgrass Genome: Tools and Strategies. The Plant Genome Journal 4 (3).
578 doi:10.3835/plantgenome2011.10.0026
- 579 Challinor AJ, Watson J, Lobell DB, Howden SM, Smith DR, Chhetri N (2014) A meta-analysis
580 of crop yield under climate change and adaptation. Nature Climate Change 4 (4):287-291.
581 doi:10.1038/nclimate2153
- 582 Christensen SA, Huffaker A, Sims J, Hunter CT, Block A, Vaughan MM, Willett D, Romero M,
583 Mylroie JE, Williams WP, Schmelz EA (2018) Fungal and herbivore elicitation of the
584 novel maize sesquiterpenoid, zealexin A4, is attenuated by elevated CO₂. Planta 247
585 (4):863-873. doi:10.1007/s00425-017-2830-5
- 586 Ciura J, Szeliga M, Grzesik M, Tyrka M (2017) Next-generation sequencing of representational
587 difference analysis products for identification of genes involved in diosgenin biosynthesis
588 in fenugreek (*Trigonella foenum-graecum*). Planta 245 (5):977-991. doi:10.1007/s00425-
589 017-2657-0
- 590 Ding Y, Northen TR, Khalil A, Huffaker A, Schmelz EA (2021) Getting back to the grass roots:
591 harnessing specialized metabolites for improved crop stress resilience. Curr Opin Biotech
592 70:174-186. doi:10.1016/j.copbio.2021.05.010
- 593 Dührkop K, Nothias L-F, Fleischauer M, Reher R, Ludwig M, Hoffmann MA, Petras D, Gerwick
594 WH, Rousu J, Dorrestein PC, Böcker S (2021) Systematic classification of unknown

- 595 metabolites using high-resolution fragmentation mass spectra. *Nature Biotechnology* 39
596 (4):462-471. doi:10.1038/s41587-020-0740-8
- 597 El Babili F, Moulis C, Bon M, Respaud M-J, Fourasté I (1998) Three furano-diterpenes from the
598 bark of *Croton campestris*. *Phytochemistry* 48 (1):165-169
- 599 Fujimatsu T, Endo K, Yazaki K, Sugiyama A (2020) Secretion dynamics of soyasaponins in
600 soybean roots and effects to modify the bacterial composition. *Plant direct* 4 (9):e00259
- 601 Gai Z, Wang Y, Ding Y, Qian W, Qiu C, Xie H, Sun L, Jiang Z, Ma Q, Wang L, Ding Z (2020)
602 Exogenous abscisic acid induces the lipid and flavonoid metabolism of tea plants under
603 drought stress. *Scientific Reports* 10 (1):12275. doi:10.1038/s41598-020-69080-1
- 604 Hamrouni I, Salah HB, Marzouk B (2001) Effects of water-deficit on lipids of safflower aerial
605 parts. *Phytochemistry* 58 (2):277-280
- 606 Horie K, Inoue Y, Sakai M, Yao Q, Tanimoto Y, Koga J, Toshima H, Hasegawa M (2015)
607 Identification of UV-Induced Diterpenes Including a New Diterpene Phytoalexin,
608 Phytocassane F, from Rice Leaves by Complementary GC/MS and LC/MS Approaches. *J*
609 *Agric Food Chem* 63 (16):4050-4059. doi:10.1021/acs.jafc.5b00785
- 610 Kim D, Paggi JM, Park C, Bennett C, Salzberg SL (2019a) Graph-based genome alignment and
611 genotyping with HISAT2 and HISAT-genotype. *Nature Biotechnology* 37 (8):907-915.
612 doi:10.1038/s41587-019-0201-4
- 613 Kim KS, Park SH, Kim DK, Jenks MA (2007) Influence of Water Deficit on Leaf Cuticular Waxes
614 of Soybean (*Glycine max* [L.] Merr.). *International Journal of Plant Sciences* 168 (3):307-
615 316. doi:10.1086/510496
- 616 Kim W, Iizumi T, Nishimori M (2019b) Global Patterns of Crop Production Losses Associated
617 with Droughts from 1983 to 2009. *Journal of Applied Meteorology and Climatology* 58
618 (6):1233-1244. doi:10.1175/JAMC-D-18-0174.1
- 619 Kind T, Liu K-H, Lee DY, DeFelice B, Meissen JK, Fiehn O (2013) LipidBlast in silico tandem
620 mass spectrometry database for lipid identification. *Nat Methods* 10 (8):755-758.
621 doi:10.1038/nmeth.2551
- 622 Lee ST, Mitchell RB, Wang Z, Heiss C, Gardner DR, Azadi P (2009) Isolation, Characterization,
623 and Quantification of Steroidal Saponins in Switchgrass (*Panicum virgatum* L.). *Journal*
624 *of Agricultural and Food Chemistry* 57 (6):2599-2604. doi:10.1021/jf803907y
- 625 Li X, Jones AD, Last RL (2020) Switchgrass metabolomics reveals striking genotypic and
626 developmental differences in saponins. bioRxiv:2020.2006.2001.127720.
627 doi:10.1101/2020.06.01.127720
- 628 Liu T-Y, Chen M-X, Zhang Y, Zhu F-Y, Liu Y-G, Tian Y, Fernie AR, Ye N, Zhang J (2019)
629 Comparative metabolite profiling of two switchgrass ecotypes reveals differences in
630 drought stress responses and rhizosheath weight. *Planta* 250 (4):1355-1369
- 631 Liu T-Y, Ye N, Wang X, Das D, Tan Y, You X, Long M, Hu T, Dai L, Zhang J, Chen M-X (2021)
632 Drought stress and plant ecotype drive microbiome recruitment in switchgrass rhizosheath.
633 *Journal of Integrative Plant Biology* n/a (n/a). doi:10.1111/jipb.13154
- 634 Liu Y, Zhang X, Tran H, Shan L, Kim J, Childs K, Ervin EH, Frazier T, Zhao B (2015) Assessment
635 of drought tolerance of 49 switchgrass (*Panicum virgatum*) genotypes using physiological
636 and morphological parameters. *Biotechnology for Biofuels* 8 (1):152. doi:10.1186/s13068-
637 015-0342-8
- 638 Liu Z, Cheema J, Vigouroux M, Hill L, Reed J, Paajanen P, Yant L, Osbourn A (2020) Formation
639 and diversification of a paradigm biosynthetic gene cluster in plants. *Nature*
640 *Communications* 11 (1):5354. doi:10.1038/s41467-020-19153-6

- 641 Lovell JT, MacQueen AH, Mamidi S, Bonnette J, Jenkins J, Napier JD, Sreedasyam A, Healey A,
642 Session A, Shu S, Barry K, Bonos S, Boston L, Daum C, Deshpande S, Ewing A,
643 Grabowski PP, Haque T, Harrison M, Jiang J, Kudrna D, Lipzen A, Pendergast TH, Plott
644 C, Qi P, Saski CA, Shakirov EV, Sims D, Sharma M, Sharma R, Stewart A, Singan VR,
645 Tang Y, Thibivillier S, Webber J, Weng X, Williams M, Wu GA, Yoshinaga Y, Zane M,
646 Zhang L, Zhang J, Behrman KD, Boe AR, Fay PA, Fritschi FB, Jastrow JD, Lloyd-Reilley
647 J, Martínez-Reyna JM, Matamala R, Mitchell RB, Rouquette FM, Ronald P, Saha M,
648 Tobias CM, Udvardi M, Wing RA, Wu Y, Bartley LE, Casler M, Devos KM, Lowry DB,
649 Rokhsar DS, Grimwood J, Juenger TE, Schmutz J (2021) Genomic mechanisms of climate
650 adaptation in polyploid bioenergy switchgrass. *Nature* 590 (7846):438-444.
651 doi:10.1038/s41586-020-03127-1
- 652 Lovell JT, Schwartz S, Lowry DB, Shakirov EV, Bonnette JE, Weng X, Wang M, Johnson J,
653 Sreedasyam A, Plott C, Jenkins J, Schmutz J, Juenger TE (2016) Drought responsive gene
654 expression regulatory divergence between upland and lowland ecotypes of a perennial C4
655 grass. *Genome Res* 26 (4):510-518. doi:10.1101/gr.198135.115
- 656 Lowry DB, Behrman KD, Grabowski P, Morris GP, Kiniry JR, Juenger TE (2014) Adaptations
657 between ecotypes and along environmental gradients in *Panicum virgatum*. *The American*
658 *Naturalist* 183 (5):682-692
- 659 Ma D, Sun D, Wang C, Li Y, Guo T (2014) Expression of flavonoid biosynthesis genes and
660 accumulation of flavonoid in wheat leaves in response to drought stress. *Plant Physiology*
661 *and Biochemistry* 80:60-66. doi:10.1016/j.plaphy.2014.03.024
- 662 Mafu S, Ding Y, Murphy KM, Yaacoobi O, Addison JB, Wang Q, Shen Z, Briggs SP, Bohlmann
663 J, Castro-Falcon G, Hughes CC, Betsiashvili M, Huffaker A, Schmelz EA, Zerbe P (2018)
664 Discovery, biosynthesis and stress-related accumulation of dolabradiene-derived defenses
665 in maize. *Plant Physiol.* doi:10.1104/pp.17.01351
- 666 Magwanga RO, Lu P, Kirungu JN, Lu H, Wang X, Cai X, Zhou Z, Zhang Z, Salih H, Wang K,
667 Liu F (2018) Characterization of the late embryogenesis abundant (LEA) proteins family
668 and their role in drought stress tolerance in upland cotton. *BMC Genetics* 19 (1):6.
669 doi:10.1186/s12863-017-0596-1
- 670 McCrindle R, Nakamura E, Anderson AB (1976) Constituents of *Solidago* species. Part VII.
671 Constitution and stereochemistry of the cis-clerodanes from *Solidago arguta* Ait. and of
672 related diterpenoids. *Journal of the Chemical Society, Perkin Transactions 1* (15):1590-
673 1597
- 674 McLaughlin S, Bouton J, Bransby D, Conger B, Ocumpaugh W, Parrish D, Taliaferro C, Vogel
675 K, Wullschlegel S (1999) Developing switchgrass as a bioenergy crop. *Perspectives on*
676 *new crops and new uses* 56:282-299
- 677 Meyer E, Aspinwall MJ, Lowry DB, Palacio-Mejía JD, Logan TL, Fay PA, Juenger TE (2014)
678 Integrating transcriptional, metabolomic, and physiological responses to drought stress and
679 recovery in switchgrass (*Panicum virgatum* L.). *BMC Genomics* 15 (1):527.
680 doi:10.1186/1471-2164-15-527
- 681 Moradi P, Mahdavi A, Khoshkam M, Iriti M (2017) Lipidomics Unravels the Role of Leaf Lipids
682 in Thyme Plant Response to Drought Stress. *International Journal of Molecular Sciences*
683 18 (10):2067
- 684 Morrow WR, Gopal A, Fitts G, Lewis S, Dale L, Masanet E (2014) Feedstock loss from drought
685 is a major economic risk for biofuel producers. *Biomass and Bioenergy* 69:135-143.
686 doi:10.1016/j.biombioe.2014.05.006

- 687 Muchlinski A, Chen X, Lovell JT, Köllner TG, Pelot KA, Zerbe P, Ruggiero M, Callaway Iii L,
688 Laliberte S, Chen F (2019) Biosynthesis and Emission of Stress-Induced Volatile Terpenes
689 in Roots and Leaves of Switchgrass (*Panicum virgatum* L.). *Frontiers in plant science*
690 10:1144
- 691 Muchlinski A, Jia M, Tiedge K, Fell JS, Pelot KA, Chew L, Davisson D, Chen Y, Siegel J, Lovell
692 JT, Zerbe P (2021) Cytochrome P450-catalyzed biosynthesis of furanoditerpenoids in the
693 bioenergy crop switchgrass (*Panicum virgatum* L.). *The Plant Journal* n/a (n/a).
694 doi:10.1111/tpj.15492
- 695 Munné-Bosch S, Alegre L (2003) Drought-Induced Changes in the Redox State of α -Tocopherol,
696 Ascorbate, and the Diterpene Carnosic Acid in Chloroplasts of Labiatae Species Differing
697 in Carnosic Acid Contents. *Plant Physiology* 131 (4):1816-1825.
698 doi:10.1104/pp.102.019265
- 699 Murphy KM, Edwards J, Louie KB, Bowen BP, Sundaresan V, Northen TR, Zerbe P (2021)
700 Bioactive diterpenoids impact the composition of the root-associated microbiome in maize
701 (*Zea mays*). *Scientific Reports* 11 (1):333. doi:10.1038/s41598-020-79320-z
- 702 Murphy KM, Zerbe P (2020) Specialized diterpenoid metabolism in monocot crops: Biosynthesis
703 and chemical diversity. *Phytochemistry* 172:112289.
704 doi:10.1016/j.phytochem.2020.112289
- 705 Nakayasu M, Ohno K, Takamatsu K, Aoki Y, Yamazaki S, Takase H, Shoji T, Yazaki K,
706 Sugiyama A (2021) Tomato roots secrete tomatine to modulate the bacterial assemblage of
707 the rhizosphere. *Plant Physiology* 186 (1):270-284
- 708 Nasrollahi V, Mirzaie-asl A, Piri K, Nazeri S, Mehrabi R (2014) The effect of drought stress on
709 the expression of key genes involved in the biosynthesis of triterpenoid saponins in
710 liquorice (*Glycyrrhiza glabra*). *Phytochemistry* 103:32-37.
711 doi:10.1016/j.phytochem.2014.03.004
- 712 Newbery F, Qi A, Fitt BD (2016) Modelling impacts of climate change on arable crop diseases:
713 progress, challenges and applications. *Curr Opin Plant Biol* 32:101-109.
714 doi:10.1016/j.pbi.2016.07.002
- 715 Olvera-Carrillo Y, Campos F, Reyes JL, Garcarrubio A, Covarrubias AA (2010) Functional
716 Analysis of the Group 4 Late Embryogenesis Abundant Proteins Reveals Their Relevance
717 in the Adaptive Response during Water Deficit in *Arabidopsis*. *Plant Physiology* 154
718 (1):373-390. doi:10.1104/pp.110.158964
- 719 Pang Z, Chong J, Zhou G, de Lima Morais DA, Chang L, Barrette M, Gauthier C, Jacques P-É, Li
720 S, Xia J (2021) MetaboAnalyst 5.0: narrowing the gap between raw spectra and functional
721 insights. *Nucleic Acids Research* 49 (W1):W388-W396. doi:10.1093/nar/gkab382
- 722 Park HL, Lee SW, Jung KH, Hahn TR, Cho MH (2013) Transcriptomic analysis of UV-treated
723 rice leaves reveals UV-induced phytoalexin biosynthetic pathways and their regulatory
724 networks in rice. *Phytochemistry* 96:57-71. doi:10.1016/j.phytochem.2013.08.012
- 725 Pelot KA, Chen R, Hagelthorn DM, Young CA, Addison JB, Muchlinski A, Tholl D, Zerbe P
726 (2018) Functional Diversity of Diterpene Synthases in the Biofuel Crop Switchgrass. *Plant*
727 *Physiology* 178 (1):54-71. doi:10.1104/pp.18.00590
- 728 Pinto AC, Garcez WS, Queiroz PP, Fiorani NG (1994) Clerodanes and tetranorclerodane from
729 *Vellozia bicolor*. *Phytochemistry* 37 (4):1115-1117
- 730 Pokhrel Y, Felfelani F, Satoh Y, Boulange J, Burek P, Gädeke A, Gerten D, Gosling SN, Grillakis
731 M, Gudmundsson L, Hanasaki N, Kim H, Koutroulis A, Liu J, Papadimitriou L, Schewe J,
732 Müller Schmied H, Stacke T, Telteu C-E, Thiery W, Veldkamp T, Zhao F, Wada Y (2021)

- 733 Global terrestrial water storage and drought severity under climate change. *Nature Climate*
734 *Change* 11 (3):226-233. doi:10.1038/s41558-020-00972-w
- 735 Posé D, Castanedo I, Borsani O, Nieto B, Rosado A, Taconnat L, Ferrer A, Dolan L, Valpuesta V,
736 Botella MA (2009) Identification of the *Arabidopsis* *dry2/sqe1-5* mutant reveals a central
737 role for sterols in drought tolerance and regulation of reactive oxygen species. *The Plant*
738 *Journal* 59 (1):63-76. doi:10.1111/j.1365-313X.2009.03849.x
- 739 Puente-Garza CA, Meza-Miranda C, Ochoa-Martínez D, García-Lara S (2017) Effect of in vitro
740 drought stress on phenolic acids, flavonols, saponins, and antioxidant activity in *Agave*
741 *salmiana*. *Plant physiology and biochemistry* 115:400-407
- 742 Quartacci MF, Pinzino C, Sgherri CL, Navari-Izzo F (1995) Lipid composition and protein
743 dynamics in thylakoids of two wheat cultivars differently sensitive to drought. *Plant*
744 *Physiology* 108 (1):191-197
- 745 Savary S, Willocquet L, Pethybridge SJ, Esker P, McRoberts N, Nelson A (2019) The global
746 burden of pathogens and pests on major food crops. *Nature Ecology & Evolution* 3 (3):430-
747 +. doi:10.1038/s41559-018-0793-y
- 748 Schmelz EA, Huffaker A, Sims JW, Christensen SA, Lu X, Okada K, Peters RJ (2014)
749 Biosynthesis, elicitation and roles of monocot terpenoid phytoalexins. *Plant J* 79 (4):659-
750 678. doi:10.1111/tbj.12436
- 751 Swaminathan S, Morrone D, Wang Q, Fulton DB, Peters RJ (2009) CYP76M7 Is an *ent*-
752 *Cassadiene* C11 α -Hydroxylase Defining a Second Multifunctional Diterpenoid
753 Biosynthetic Gene Cluster in Rice. *The Plant Cell* 21 (10):3315-3325.
754 doi:10.1105/tpc.108.063677
- 755 Tiedge K, Muchlinski A, Zerbe P (2020) Genomics-enabled analysis of specialized metabolism in
756 bioenergy crops: current progress and challenges. *Synthetic Biology* 5 (1):ysaa005
- 757 Vaughan MM, Christensen S, Schmelz EA, Huffaker A, McAuslane HJ, Alborn HT, Romero M,
758 Allen LH, Teal PE (2015a) Accumulation of terpenoid phytoalexins in maize roots is
759 associated with drought tolerance. *Plant, cell & environment* 38 (11):2195-2207
- 760 Vaughan MM, Christensen S, Schmelz EA, Huffaker A, McAuslane HJ, Alborn HT, Romero M,
761 Allen LH, Teal PE (2015b) Accumulation of terpenoid phytoalexins in maize roots is
762 associated with drought tolerance. *Plant Cell Environ* 38 (11):2195-2207.
763 doi:10.1111/pce.12482
- 764 Yao L, Cheng X, Gu Z, Huang W, Li S, Wang L, Wang YF, Xu P, Ma H, Ge X (2018) The
765 AWP19 Family Protein OsPM1 Mediates Abscisic Acid Influx and Drought Response
766 in Rice. *Plant Cell* 30 (6):1258-1276. doi:10.1105/tpc.17.00770
- 767 Zhang Q, Liu H, Wu X, Wang W (2020) Identification of drought tolerant mechanisms in a
768 drought-tolerant maize mutant based on physiological, biochemical and transcriptomic
769 analyses. *BMC Plant Biology* 20 (1):315-315. doi:10.1186/s12870-020-02526-w

770

771 **Figure legends**

772 **Fig. 1: Left panel:** Photographs of Alamo and Cave-in-Rock plants after four weeks of drought
773 treatment (+d) or normal watering (-d). **Right panels:** Volcano plots of differentially expressed

774 genes identified after four weeks of drought in (a) Alamo leaves (b) Cave-in-Rock leaves (c)
775 Alamo roots (d) Cave-in-Rock roots. Differential expression threshold: $\text{padj} < 0.05$, $\log_2 \text{FC}$, and
776 > 1 .

777 **Fig. 2:** KEGG pathway enrichment analysis of differentially expressed genes. Circle color denotes
778 the adjusted p -value (Padj), circle size is proportional to the number of genes involved in the
779 enrichment of the pathway (Count).

780 **Fig. 3:** Plot of normalized gene expression profiles of genes with predicted functions in (a)
781 terpenoid backbone biosynthesis and (b) flavonoid backbone biosynthesis after 0, 2 or 4 weeks in
782 drought-treated (D) or well-watered control (C) Alamo and Cave-in-Rock (CiR) plants. Gene
783 expression data are based on four biological replicates and gene functional annotations are based
784 on best matches in BLAST searches against public and in-house protein databases. Gene IDs were
785 derived from the *Panicum virgatum* genome v5.1 (phytozome-
786 next.jgi.doe.gov/info/Pvirgatum_v5_1). Abbreviations: *DXS*, 1-deoxyxylulose 5-phosphate
787 synthase; *DXR*, 1-deoxyxylulose 5-phosphate reductase; *HMGR*, HMG-CoA reductase; *FPPS*,
788 farnesyl pyrophosphate synthase; *GGPPS*, geranylgeranyl pyrophosphate synthase; *SQS*,
789 squalene synthase; *SQE*, squalene epoxidase; *PAL*, phenylalanine ammonia lyase; *C4H*,
790 cinnamate-4-hydroxylase; *4CL*, 4-coumaroyl-CoA ligase; *CHS*, chalcone synthase; *CHI*,
791 chalcone isomerase.

792

793 **Fig. 4:** Hierarchical cluster analysis of select genes with predicted functions in triterpenoid
794 biosynthesis in Alamo and Cave-in-Rock. Gene functional annotations are based on best matches
795 in BLAST searches against in-house protein databases of known triterpenoid-metabolic genes.

796 Gene IDs are derived from the *Panicum virgatum* genome v5.1 (phytozome-
797 next.jgi.doe.gov/info/Pvirgatum_v5_1). Gene expression data are based on four biological
798 replicates. Dashed boxes highlight genes with relevant co-expression patterns. Right side: C0L,
799 C2L, C4L: Leaves of well-watered control plants after 0, 2 and 4 weeks of treatment; C0R, C2R,
800 C4R: Roots of well-watered control plants; D0L, D2L, D4L: Leaves of drought-stressed plants;
801 D0R, D2R, D4R: Roots of drought-stressed plants.

802

803 **Fig. 5:** Hierarchical cluster analysis of select genes with known or predicted functions in
804 diterpenoid biosynthesis in Alamo and Cave-in-Rock. Gene functional annotations are based on
805 previous biochemical enzyme characterizations or best matches in BLAST searches against in-
806 house protein databases of known diterpenoid-metabolic genes. Gene IDs are derived from the
807 *Panicum virgatum* genome v5.1 (phytozome-next.jgi.doe.gov/info/Pvirgatum_v5_1). Gene
808 expression data are based on four biological replicates. Dashed boxes highlight genes with relevant
809 co-expression patterns. C0L, C2L, C4L: Leaves of well-watered control plants after 0, 2 and 4

810 weeks of treatment; C0R, C2R, C4R: Roots of well-watered control plants; D0L, D2L, D4L:
811 Leaves of drought-stressed plants; D0R, D2R, D4R: Roots of drought-stressed plants.

812

813 **Fig. 6:** Partial Least-Squares Discriminant Analysis (PLS-DA) plots of LC-MS positive mode
814 metabolome divergence based on five biological replicates. X-axis: Principal Component 1; y-
815 axis: Principal Component 2.

816

817 **Fig. 7:** Scree plot of metabolite features obtained via LC-MS positive mode analysis that show the
818 most significant contribution to changes in metabolite profiles in response to drought stress. A
819 higher coefficient (x-axis) denotes a higher importance for this feature in the Partial Least-Squares
820 Discriminant Analysis (PLS-DA) shown in Fig. 6. Boxes display the relative abundance of a
821 feature among the different groups as based on five biological replicates. Metabolite annotations
822 are based on matching m/z ratios, RT and fragmentation patterns against online databases.

823

824 **Fig. 8: (a)** Hierarchical cluster analysis of select specialized metabolite accumulation patterns.
825 Sucrose and abscisic acid (ABA) abundance provide as drought-related reference metabolites.
826 Metabolite annotations are based on matching m/z ratios, RT and fragmentation patterns against
827 online databases. **(b)** Structures of drought-induced diterpenoids, 15,16-epoxy-2-oxo-5 α 8 α -
828 cleroda-3,13(16),14-triene (m/z 301, panicoloid A), 15,16-epoxy-2-oxo-5 β 8 α -cleroda-
829 3,13(16),14-triene (m/z 301, panicoloid B) and 2-oxo-5 α 8 α -cleroda-3,13-dien-16,15-olide (m/z

830 317, panicoloid C), isolated from drought-stressed switchgrass roots. Metabolite abundance is
831 based on five biological replicates.

832

833 **Supporting Information**

834 **Fig. S1:** Available water content (AWC) in the soil during the treatment

835 **Fig. S2:** Differentially expressed genes between all groups after four weeks of drought treatment

836 **Fig. S3:** Identification of significantly enriched metabolic pathways at the end of the treatment via
837 GO term analysis

838 **Fig. S4:** LC-MS chromatograms and spectra of identified panicoloids

839 **Fig. S5:** Diterpenoid network in switchgrass

840 **Fig. S6:** NMR analysis of panicoloids A-C

841 **Table S1:** Complete list of differentially expressed genes (DEGs)

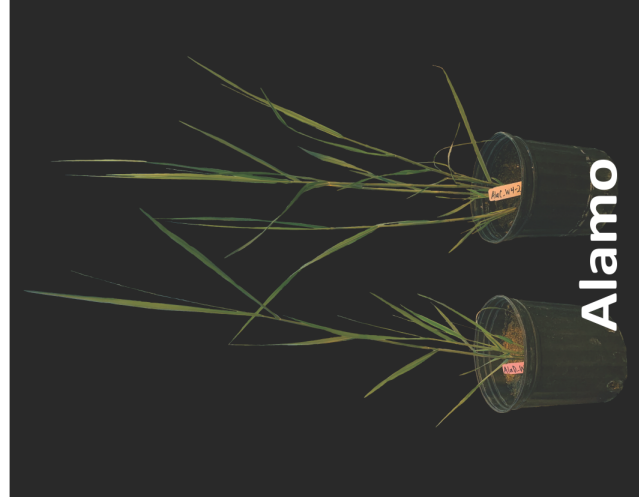
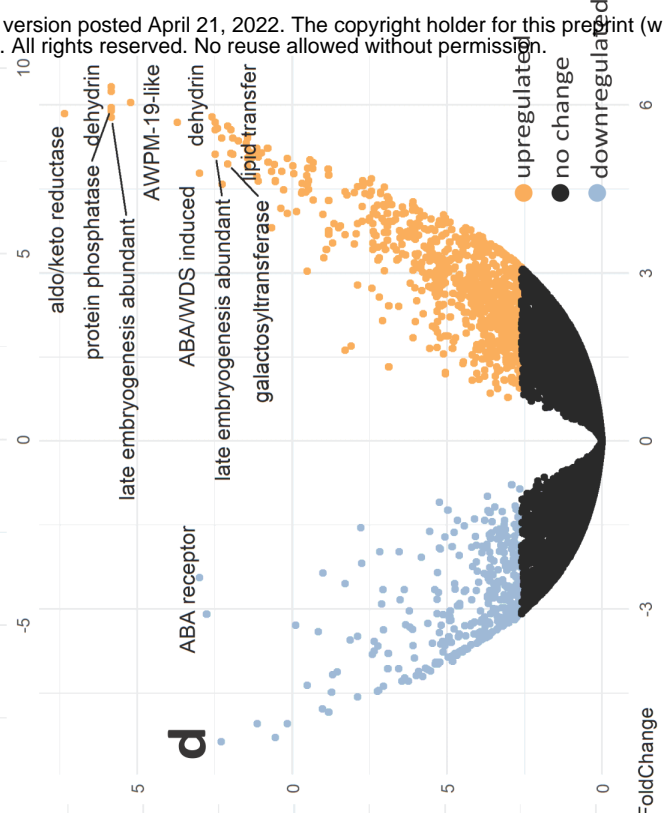
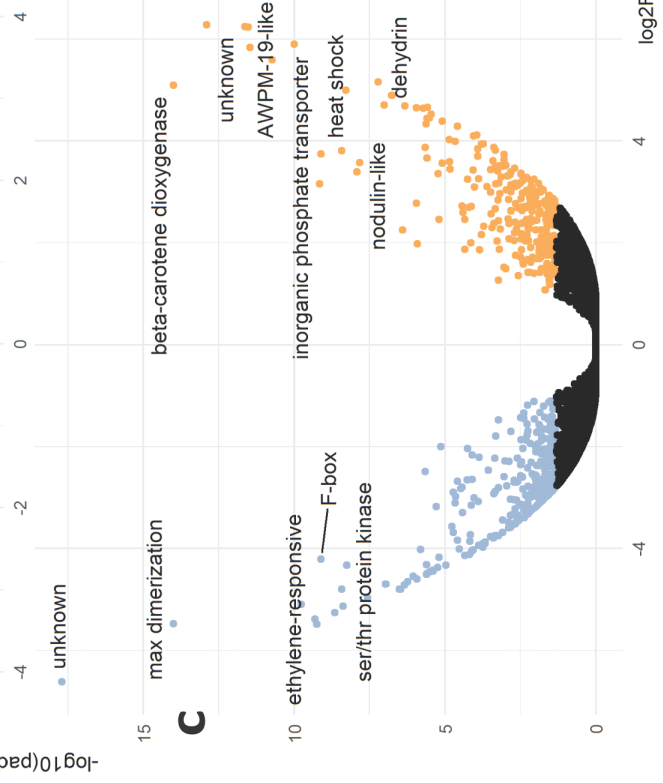
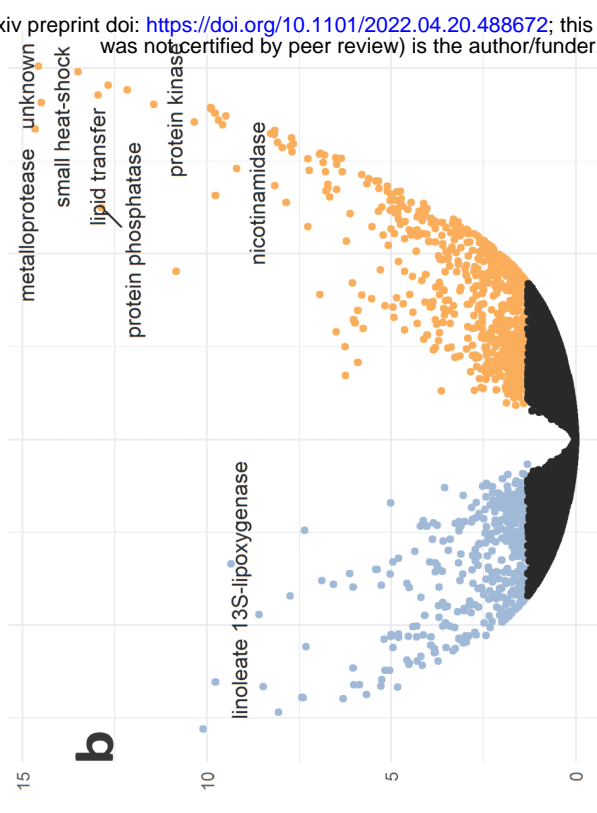
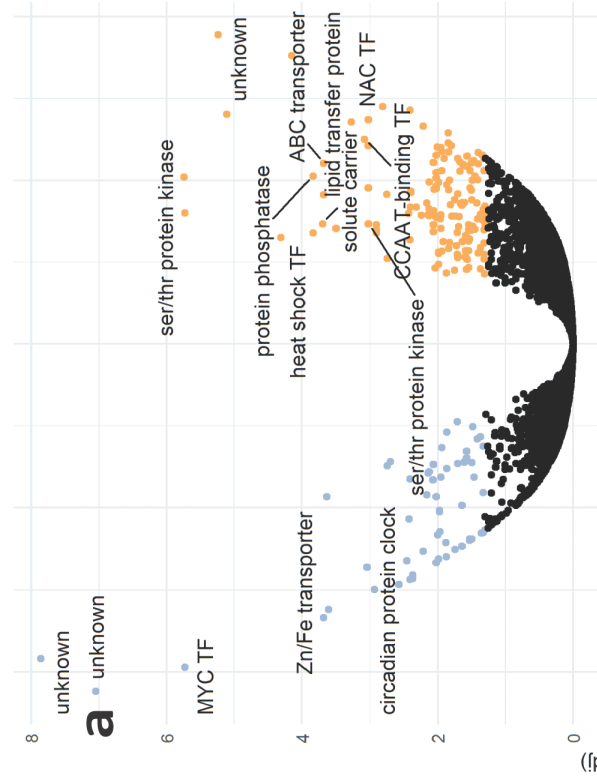
842 **Table S2:** Permutational multivariate analysis of variance (PERMANOVA) of a) gene expression
843 levels and b) metabolite abundances

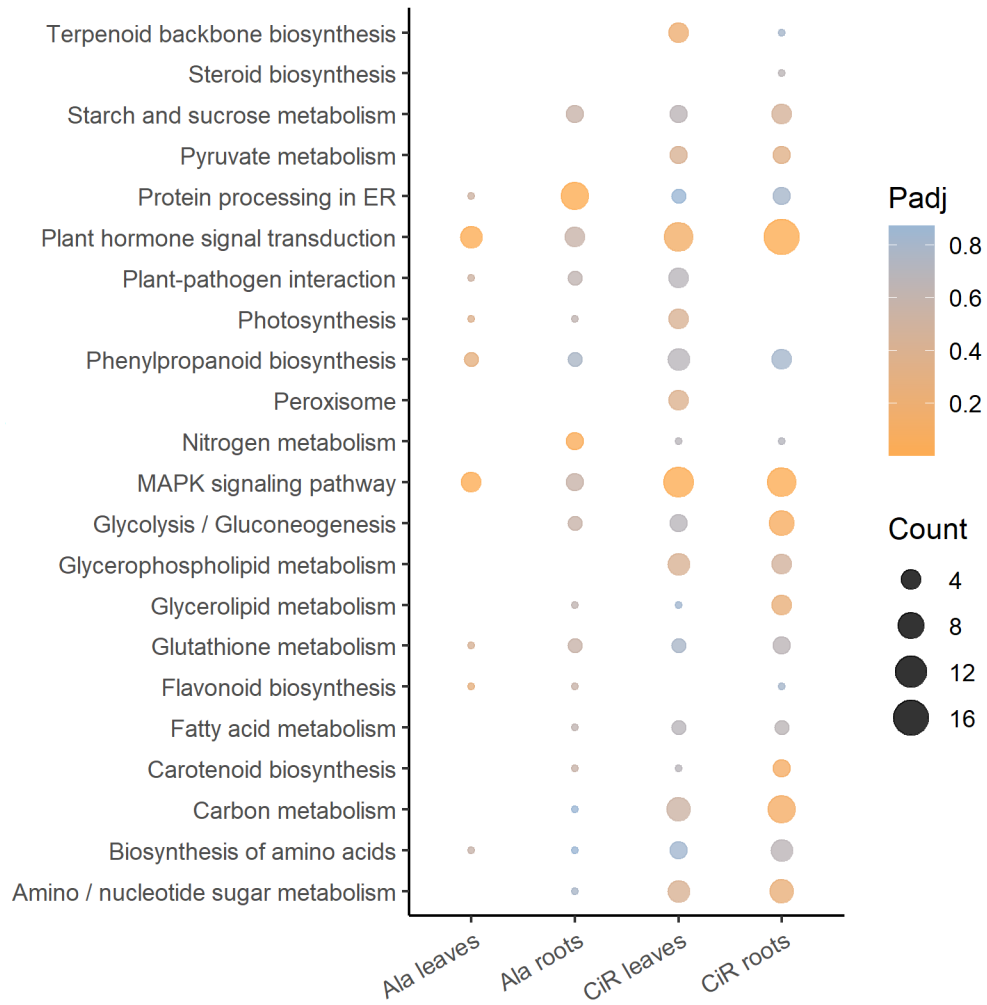
844 **Table S3:** Enrichment of GO terms and KEGG pathways in Alamo and Cave-in-Rock

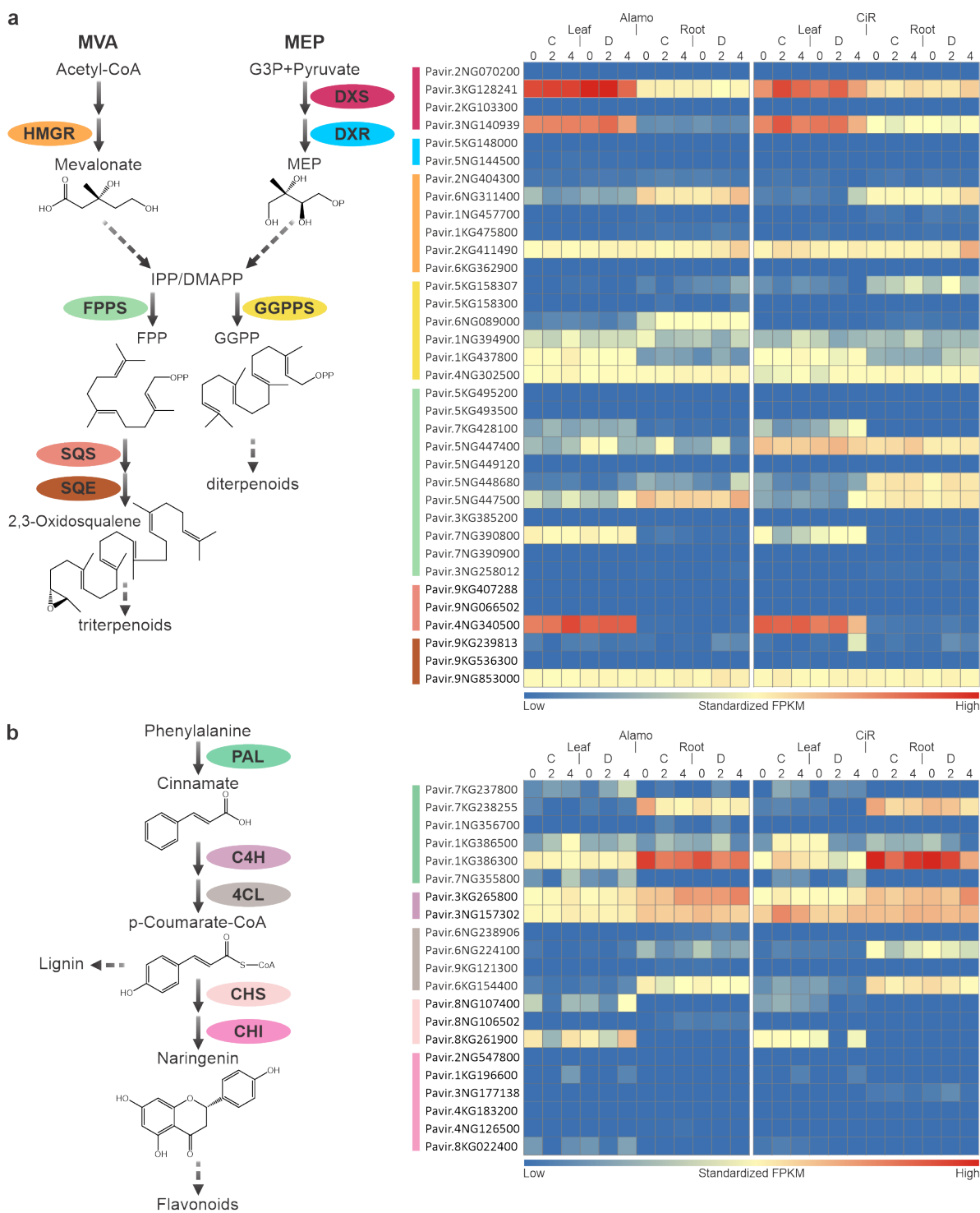
845 **Table S4:** Complete list of the calculated FPKM (Fragments Per Kilobase of transcript per Million
846 mapped reads) values for all genes

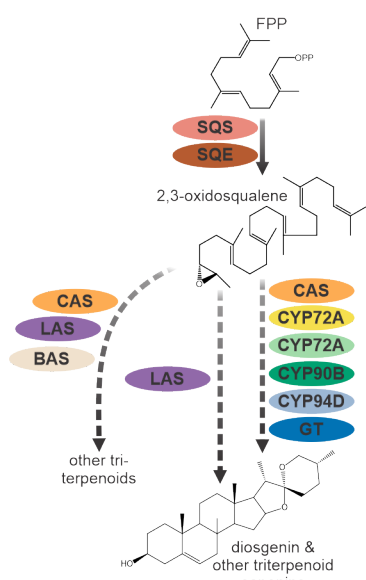
847 **Table S5:** List of all mass features from the positive mode LC-MS dataset that were selected for
848 the downstream statistical analysis.

849 **Table S6:** Statistical analysis for detected LC-MS features of annotated specialized metabolites

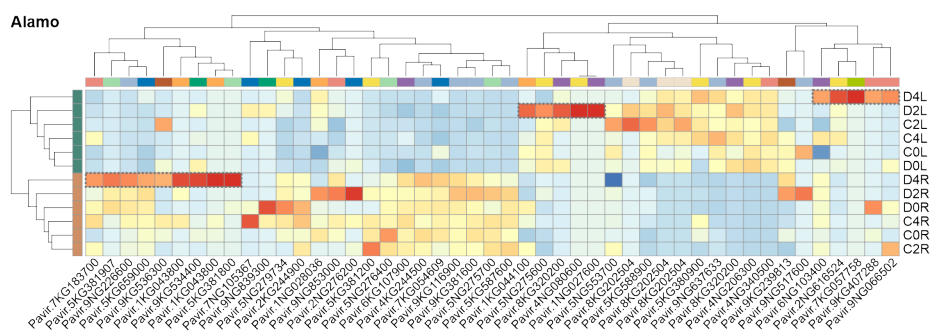




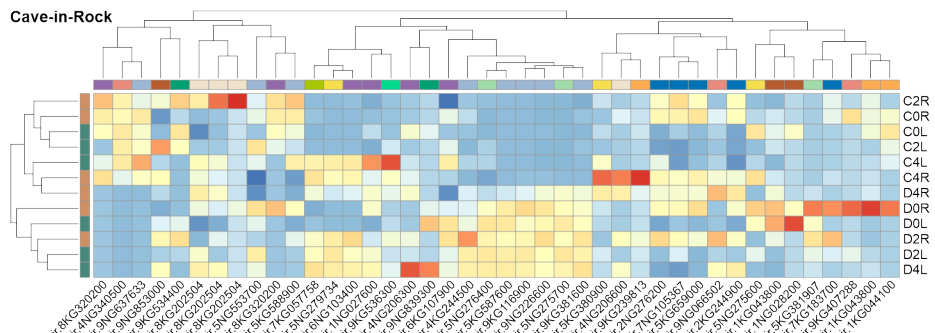


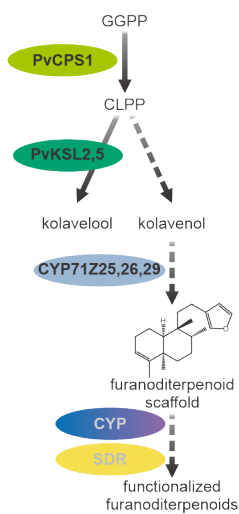


Alamo

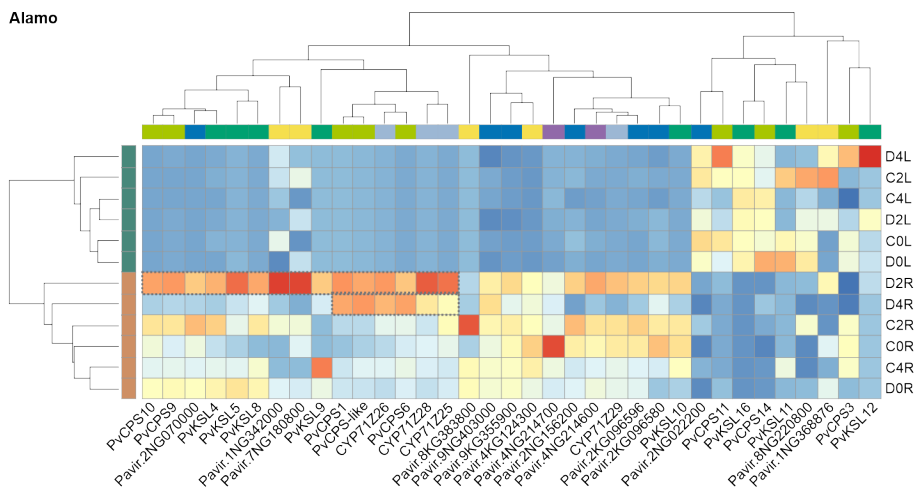


Cave-in-Rock

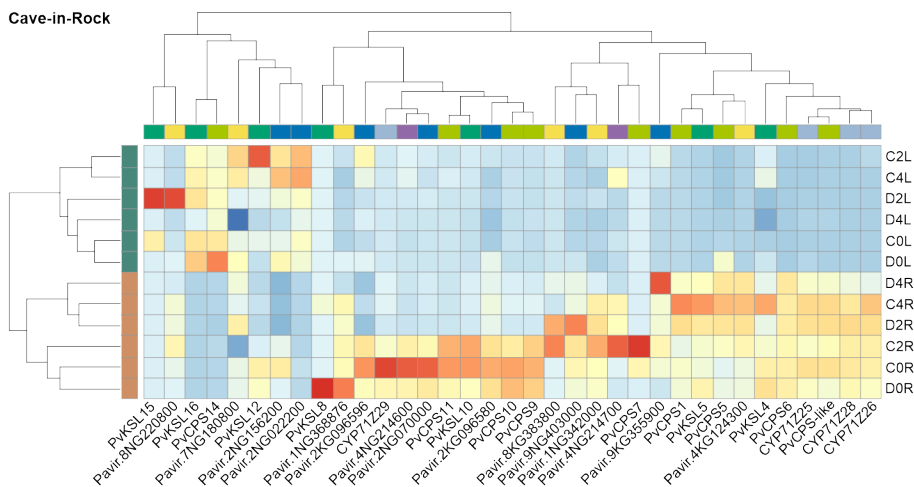




Alamo



Cave-in-Rock



Tissue Gene family
 leaves class II diTPS class I diTPS CYP701 CYP71Z CYP99
 roots short-chain alcohol dehydrogenase/reductase-like

Low Standardized FPKM High

